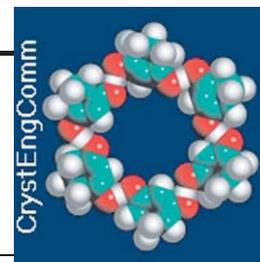# Metal–organic framework structures of Cu(II) with pyridine-2,6-dicarboxylate and different spacers: identification of a metal bound acyclic water tetramer

Sujit K. Ghosh,[a] Joan Ribas*[b] and Parimal K. Bharadwaj*[a]

[a]Department of Chemistry, Indian Institute of Technology Kanpur, 208016, India
[b]Department de Quimica Inorganica, Universitat de Barcelona, Diagonal 647, 08028 Barcelona, Spain. E-mail: pkb@iitk.ac.in; joan.ribas@qi.ub.es

The ligand pyridine-2,6-dicarboxylic acid (pdcH$_2$) reacts under hydrothermal conditions, with Cu(NO$_3$)$_2$·6H$_2$O in the presence of different N-heterocycles used as spacers to form 1D, 2D or 3D metal–organic framework structures depending on the nature of the spacer. These network structures are characterized by X-ray crystallography, variable temperature magnetic measurements, powder X-ray diffraction, infrared and thermal gravimetric analyses. With 4,4′-bipyridine spacer, a 2D network is formed where every alternate Cu(II) ion in the chain is coordinated terminally to an acyclic tetrameric water cluster.

Introduction

The design and synthesis of metal–organic framework (MOF) structures have received enormous attention[1–5] in recent years due to their potential applications in diverse areas such as catalysis, optoelectronics, supramolecular storage of molecules, molecular magnetism and so on. Formation of these structures depends[6] on several factors which are: (i) stereo-electronic molecular information encoded in the ligand(s); (ii) reading-out this information by metal ions having a set of coordination numbers and stereochemical preferences depending on their size, charge and electronic structures; and (iii) the external conditions used for the recognition and its expression in the final supramolecular entities. When two or more different ligands are used, their design and choice must fulfil the criteria for spontaneously generating well-defined architectures. Metal–organic hybrid structures of paramagnetic metal ions are particularly interesting, as these may give rise to a series of novel framework structures with potential applications in the fields of molecular magnetism[7] and materials chemistry.[8] A commonly used strategy in building such extended network structures is to employ bridging ligands capable of transmitting magnetic interactions in addition to propagating the network. In the present work, we used pyridine-2,6-dicarboxylate (pdc^{2-}) as a chelating ligand. This ligand has limited steric hindrance and weak stacking interactions and can offer possibilities to form homoleptic coordination polymers[9] through carboxylate bridging. The compounds **1** and **2** were prepared using 4,4′-bipyridine and pyrazine as spacers. These two ligands have been employed[10–12] by various workers in the field for the construction of coordination polymeric structures. Compound **3** was made using pyridine as a co-ligand to engineer a 1D coordination polymer as it has no scope for acting as a bridging ligand. Transition metal 1D coordination polymers[13] have been reported earlier in the literature.

Interestingly, when 4,4′-bipyridine is used as the spacer, every alternate Cu(II) ion is bound to an acyclic water tetrameric cluster. Hydrogen-bonding interactions and their fluctuations determine the properties of water although they still remain as ill-understood phenomena.[14] The present upsurge[15–18] in studying small water clusters in crystal hydrates is aimed not only at understanding the "anomalous" behavior of bulk water but also in probing its possible role(s) in the stabilization and functioning of biomolecules and in designing new materials. The existence of a quasi-planar cyclic tetramer was shown[19] experimentally by vibration rotation tunneling (VRT) spectroscopy. Similar structures have been inferred from several theoretical studies[20,21] and identified[22,23] in inorganic–organic hybrid or organic host lattices. The present contribution reports the synthesis, crystal structure, thermal stability and variable temperature magnetic properties of the three new copper containing MOFs.

Experimental section

Materials

Pyridine-2,6-dicarboxylic acid (pdcH$_2$), 4,4′-bipyridine (4,4′-bipy) and pyrazine (pyz) were from Aldrich while pyridine (py) and Cu(NO$_3$)$_2$.6H$_2$O were from SD Fine Chemicals, India. All the chemicals were used as received.

Physical measurements

Spectroscopic data were collected as follows: IR (KBr disk, 400–4000 cm^{-1}) Perkin-Elmer Model 1320; X-ray powder pattern (Cu Kα radiation at a scan rate of 3° min^{-1}, 293 K) Siefert ISODEBYEFLEX-2002 X-ray generator; thermogravimetric analysis (heating rate of 5 °C min^{-1}) Perkin-Elmer Pyris 6. The magnetic studies were carried out on crystalline samples of **1**, **2** and **3** on a SQUID magnetometer in the temperature range of 2–300 K at an applied field of 0.1 T. Diamagnetic corrections were estimated[7a] from Pascal's Table. Microanalyses for the compounds were obtained from CDRI, Lucknow.

Synthesis of {Cu$_2$(pdc)$_2$(4,4′-bpy)·4H$_2$O}$_n$ (1)

A solution of Cu(NO$_3$)$_2$·6H$_2$O (1 mmol) in 5 mL H$_2$O was added to pyridine-2,6-dicarboxylic acid (1 mmol) and 4,4′-bipyridine (1 mmol) in a Teflon-lined stainless steel autoclave which was heated under autogenous pressure to 180 °C for 72 h and then allowed to cool to RT. Dark blue rectangular crystals of **1** deposited on the walls of the container, were collected and

air-dried. Yield *ca.* 45%. Anal. calcd for $C_{24}H_{22}N_4O_{12}Cu_2$: C, 44.05; H, 3.23; N, 8.17%. Found: C, 44.25; H, 3.73; N, 8.19%.

Synthesis of $Cu_2(pdc)_2(pyz)\cdot4H_2O$ (2)

This compound was isolated as blue prismatic crystals following the above procedure using pyrazine in place of 4,4′-bipyridine. Yield *ca.* 42%. Anal. calcd for $C_{18}H_{14}N_4O_{12}Cu_2$: C, 35.47; H, 2.97; N, 9.19%. Found: C, 35.52; H, 2.83; N, 9.33%.

Synthesis of $\{Cu(pdc)(py)\}_n$ (3)

This compound was isolated as blue rectangular parallelopipeds using pyridine in place of 4,4′-bipyridine in 68% yield. This compound can also be obtained in comparable yields at room temperature. Anal. calcd for $C_{12}H_8N_2O_4Cu$: C, 46.83; H, 2.62; N, 9.10%. Found: C, 46.65; H, 2.73; N, 8.89%.

X-ray structural studies

Single crystal X-ray data on **1**–**3** were collected at room temperature on an Enraf-Nonius CAD4 Mach2 X-ray diffractometer using graphite monochromated Mo Kα radiation (λ = 0.71073 Å). The cell parameters in each case were determined by least-squares refinement of the diffractometer setting angles from 25 centered reflections that were in the range, $15° \leqslant 2\theta \leqslant 20°$. Three standard reflections were measured every hour to monitor instrument and crystal stability. The linear absorption coefficients, scattering factors for the atoms, and the anomalous dispersion corrections were taken from International Tables for X-ray crystallography.[24] The structures were solved by the direct method using SIR92[25] and were refined on F^2 by full-matrix least-squares technique using the SHELXL-97[26] program package. The non-hydrogen atoms were refined anisotropically. All hydrogen atoms were located in successive difference Fourier maps and they were treated as riding atoms using SHELXL default parameters. The crystal data for the three structures are given in Table 1 while selected bond distances and angles are collected in Table 2. CCDC reference numbers 216109 (**1**), 231774 (**2**), 231775 (**3**). See http://www.rsc.org/suppdata/ce/b4/b407571d/ for crystallographic data in CIF or other electronic format.

Results and discussion

All three compounds are stable in air and are sparingly soluble in water but insoluble in common organic solvents.

The structure of **1** consists of dimeric Cu(II) in the asymmetric unit where Cu(1) is pentacoordinated with square pyramidal geometry and Cu(2) is hexacoordinated with tetragonal geometry. Each Cu(II) ion in the dimeric unit is bonded equatorially to a pdc^{2-} and a 4,4′-bipyridine ligands (N_2O_2 donor set). The equatorial Cu–N and Cu–O bond distances (Table 2) for the two copper centers differ slightly although they are within normal distances as found in the literature for tetragonal Cu(II) complexes.[13b,27] The dimeric units are connected through bridging from carboxylate O atoms to both the Cu(II) ions axially. While Cu(1) is bonded at a distance of 2.418(6) Å to a carboxylate O of Cu(2) of the neighboring dimer unit, Cu(2) is semi-coordinated at a distance of 2.768(4) Å to a carboxylate O of Cu(1) of another neighbour propagating the polymeric chain along the crystallographic *a*-axis (Fig. 1). The Cu(2) atom of the dimer is also axially coordinated to a water molecule (O4w) showing a distance of 2.353(6) Å which is slightly longer for the Jahn–Teller active metal ion. The bond angles are slightly different from the values required for an ideal square pyramidal or tetragonal geometry. The two pyridine rings of the 4,4′-bipyridine spacer are slightly out of coplanarity showing a dihedral angle of 8.69(1)°. Also, none of the pdc^{2-} ligands are coplanar with either pyridine rings of the spacer in the dimeric unit. Rectangular voids of approximate dimension 12.8 Å × 2.9 Å along the crystallographic *a*-axis can be seen. The axially coordinated O4w is hydrogen-bonded to a bent water trimer forming an overall acyclic tetrameric water cluster (Fig. 2). Each O atom of this tetramer is hydrogen-bonded to the nearest carboxylate oxygens with an average O⋯O nonbonding distance of *ca.* 2.90(6) Å extending the network approximately along the crystallographic *c*-axis (Fig. 3a).

Hydrogen-bonding interactions and their fluctuations and rearrangement dynamics determine the properties of liquid water and the roles it plays in cloud and ice formation, solution chemistry as well as in the stabilization and functioning of biomolecules. Both theoretical and experimental studies of tetrameric water clusters indicated[19–23] a quasi-planar cyclic minimum energy structure with an S_4 symmetry where each

Table 1 Crystal data and structure refinement for **1**–**3**

	1	2	3
Empirical formula	$C_{24}H_{22}Cu_2N_4O_{12}$	$C_9H_9Cu_1N_2O_6$	$C_6H_4Cu_{0.5}NO_2$
Formula weight	685.54	304.72	153.87
Temperature/K	293(2)	293(2)	293(2)
Radiation, wavelength	Mo Kα, 0.71073 Å	Mo Kα, 0.71073 Å	Mo Kα, 0.71073 Å
Crystal system	Triclinic	Monoclinic	Monoclinic
Space group	$P\bar{1}$	$P2_1/n$	$C2/c$
a/Å	7.217(5)	11.835(2)	8.082(2)
b/Å	10.605(3)	7.351(5)	13.540(5)
c/Å	17.705(2)	12.501(3)	9.999(4)
α/°	79.609(5)	90.00	90.00
β/°	83.571(5)	102.031(4)	91.87(7)
γ/°	71.787(7)	90.00	90.00
V/Å^3	1263.8(11)	1063.7(10)	1093.7(9)
Z	2	4	4
ρ_{calc}/Mg m^{-3}	1.801	1.903	0.935
μ/mm^{-1}	1.759	2.077	1.004
$F(000)$	696	616	310
Refl. collected	4452	1874	964
Independent refl.	2346	1232	817
Refinement method	Full-matrix least- squares on F^2	Full-matrix least- squares on F^2	Full-matrix least- squares on F^2
GooF	1.029	1.001	1.120
Final R indices	R_1 = 0.0526	R_1 = 0.0534	R_1 = 0.0318
[$I > 2\sigma(I)$]	wR_2 = 0.1326	wR_2 = 0.1396	wR_2 =0.0852
R indices	R_1 = 0.1396	R_1 = 0.0989	R_1 = 0.0414
wR_2 (all data)	0.1764	0.1640	0.0911

Table 2 Selected bond distances (Å) and bond angles (°) in **1**, **2** and **3**

1

Cu1–N1 1.898(6)	Cu1–N2 1.932(6)
Cu1–O3 1.980(5)	Cu1–O2 2.043(5)
Cu1–O5 2.418(6)	Cu2–N4 1.900(6)
Cu2–N3 1.952(6)	Cu2–O6 2.022(5)
Cu2–O7 2.033(6)	Cu2–OW4 2.353(6)
Cu2–O1 2.768(5)	
N1–Cu1–N2 173.6(3)	N1–Cu1–O3 81.6(2)
N2–Cu1–O3 97.5(2)	N1–Cu1–O2 79.8(2)
N2–Cu1–O2 100.5(2)	O3–Cu1–O2 160.9(2)
N1–Cu1–O5 85.9(2)	N2–Cu1–O5 100.4(2)
O3–Cu1–O5 95.5(2)	O2–Cu1–O5 87.6(2)
N4–Cu2–N3 172.6(3)	N4–Cu2–O6 80.5(2)
N3–Cu2–O6 97.4(2)	N4–Cu2–O7 80.0(2)
N3–Cu2–O7 101.5(2)	O6–Cu2–O7 160.1(2)
N4–Cu2–OW4 91.3(2)	N3–Cu2–OW4 95.7(3)
O6–Cu2–OW4 89.6(2)	O7–Cu2–OW4 94.4(2)
C7–O2–Cu1 115.2(5)	C1–O3–Cu1 115.7(5)
C24–O5–Cu1 110.0(5)	C24–O6–Cu2 114.4(5)
C18–O7–Cu2 114.8(5)	C6–N1–C2 122.9(7)
C6–N1–Cu1 119.5(5)	C2–N1–Cu1 117.2(5)
C8–N2–C12 116.9(7)	C8–N2–Cu1 120.3(5)
C12–N2–Cu1 122.7(5)	C17–N3–C15 117.1(7)
C17–N3–Cu2 119.1(5)	C15–N3–Cu2 123.7(5)
C19–N4–C23 121.0(7)	C19–N4–Cu2 120.1(5)
C23–N4–Cu2 118.9(5)	

2

Cu1–N1 1.896(5)	Cu1–N2 1.972(5)
Cu1–O2 2.041(5)	Cu1–O3 2.075(4)
Cu1–OW1 2.330(5)	Cu1–OW2 2.437(6)
N1–Cu1–N2 175.4(2)	N1–Cu1–O2 80.9(2)
N2–Cu1–O2 97.6(2)	N1–Cu1–O3 79.8(2)
N2–Cu1–O3 101.9(2)	O2–Cu1–O3 160.4(2)
N1–Cu1–OW1 91.5(2)	N2–Cu1–OW1 84.2(2)
O2–Cu1–OW1 91.5(2)	O3–Cu1–OW1 92.4(2)
N1–Cu1–OW2 101.9(2)	N2–Cu1–OW2 82.5(2)
O2–Cu1–OW2 94.2(2)	O3–Cu1–OW2 86.5(2)
OW1–Cu1–OW2 166.1(2)	C1–O2–Cu1 112.8(4)
C7–O3–Cu1 114.3(4)	C6–N1–C2 122.2(5)
C6–N1–Cu1 119.0(4)	C2–N1–Cu1 118.5(4)
C9–N2–C8 118.5(5)	C9–N2–Cu1 119.3(4)
C8–N2–Cu1 122.2(4)	Ow1–O3 2.903 (5)
Ow1–O1 2.769 (6)	Ow2–O4 2.908 (5)
Ow2–O4 2.829 (5)	

3

Cu1–N1 1.888(3)	Cu1–N2 1.940(3)
Cu1–O2 2.002(2)	Cu1–O2 2.003(2)
N1–Cu1–N2 180.000(1)	N1–Cu1–O2 80.92(6)
N2–Cu1–O2 99.08(6)	N1–Cu1–O2 80.89(6)
N2–Cu1–O2 99.11(6)	O2–Cu1–O2 161.81(11)
C4–O2–Cu1 115.09(18)	C3–N1–C3 123.1(3)
C3–N1–Cu1 118.45(16)	C3–N1–Cu1 118.47(16)
N2–C5–C6 123.0(3)	C5–N2–C5 117.2(4)
C5–N2–Cu1 121.37(19)	C5–N2–Cu1 121.39(19)

water molecule forms two hydrogen bonds. The average O···O distance was estimated to be 2.79 Å in the gas phase while those found in crystal lattices show a wide range of O···O distances (2.77–3.00 Å). In **1**, the water molecules are quite strongly bonded to each other as the O···O distances span the narrow range of 2.736–2.778 Å. The O···O···O angle is found to be close to 116° (Table 3). In comparison, acyclic trimeric water clusters of C_{2v} symmetry have been predicted theoretically[29] where the O···O···O angle is calculated to span the range, 116–124°. The four O atoms of the water cluster are not coplanar.

In **2**, the pyrazine spacer binds the two Cu(pdc) units forming a dimer (Fig. 4a) where the pyrazine is slightly away from coplanarity with the two pdc^{2-} ligands (dihedral angle being > 10°). The two axial sites are occupied by two water molecules showing an overall tetragonal symmetry around each Cu(II). Half of this dimer is present in the asymmetric unit. In this case, the two axial sites are occupied by two water molecules rather than bridging carboxylate O atoms as in **1**. The equatorial Cu–N and Cu–O bond distances (Table 2) are similar to those found in related structures.[13b,27] The two axial Cu–O distances are significantly longer compared to those present in other tetragonal Cu(II) complexes.[28] The bond angles around copper are significantly distorted from ideal tetragonal geometry. The uncoordinated carboxylate O atoms and the two axially bound water molecules are involved in strong intermolecular hydrogen-bonding interactions (Table 2) forming an overall 3D structure (Fig. 4b).

In **3**, a 1D coordination polymer could be engineered in the absence of a bridging co-ligand. In this structure, each metal ion is coordinated to one pdc^{2-}, one pyridine and two bridging carboxylate O atoms showing tetragonal [4 + 2] coordination. The equatorial sites are occupied by two N and two O atoms with normal Cu–O and Cu–N bond distances.[13b,27,28] The two axial sites are occupied by bridging carboxylate O atoms at a distance of 2.793(6) Å that propagate the 1D coordination polymeric chain along the crystallographic *c*-axis. The pdc^{2-} ligands (as well as the pyridine molecules) are *trans* to each other along the polymeric chain (Fig. 5) that does not allow other polymeric chains to come near to form a 2D network *via* hydrogen bonding. However, individual polymeric chains are connected in the solid state through weak hydrogen-bonding interactions involving aromatic CH and carboxylate O [C2···O1′, 3.219(1); C6···O2″, 3.445(2) Å]. The carboxylate O atoms are arranged in a staircase-like fashion along the crystallographic *b*-axis. As in the previous two cases, all bond distances and angles involving the ligand moieties are normal within statistical errors. The two axial Cu–N distances (Table 2) are comparable to known[30] axial Cu–N(pyridine) distances found in tetragonal complexes of the metal ion.

The magnetic susceptibility measurements were carried out from 300 to 2 K. The magnetic behavior of **1** is illustrated in Fig. 6 by means of a plot of $\chi_m T$ *vs.* the temperature, assuming a dinuclear entity in which copper(II) ions are linked either by *syn–anti* carboxylato bridging ligand or by 4,4′-byp bridging ligand. At 300 K, the $\chi_m T$ value is 0.93 cm^3 mol^{-1} K, as expected for two magnetically quasi-isolated copper ions.[31] Upon cooling from room temperature, the $\chi_m T$ value remains almost constant till 50 K and then sharply decreases to 0.65 cm^3 mol^{-1} K as the temperature is lowered to 2 K. Using the Hamiltonian $H = -JS_1S_2 - zJ' < S_z > S_z$ and fitting to the Bleaney–Bowers formula for a dinuclear Cu(II),[32] with the molecular field approach[31] for considering also the J' intermolecular interactions through 4,4′-bpy and hydrogen bond, the best-fit parameters found are : $J = -1.33 \pm 0.05$ cm^{-1}, $J' = -0.11$ cm^{-1}, $g = 2.22$ and $R = 2.0 \times 10^{-5}$ (R is the agreement factor defined as $\Sigma_i[(\chi_m)_{obs} - (\chi_m)_{calc}]^2/ \Sigma_i[(\chi_m)_{obs}]$. To complete and corroborate the susceptibility data, a magnetization experiment was performed at 2 K between 0 and 5 T (Fig. 6, inset). The reduced molar magnetization (for the dimer) tends to 2 Nβ when the field increases to 5 T. The simulated curve using the Brillouin formula[31] for two isolated copper(II) ions with $g = 2.22$ lies only slightly above the experimental curve, indicating negligible anti-ferromagnetic coupling, as the M/Nβ values are very sensitive to the increase of the $|J|$ value. The X-band solid-state EPR spectra of **1** do not change with temperature (from 300 to 4 K). They show typical axial pattern[33] with $g_{\parallel} = 2.26$, $g_{\perp} = 2.04$ corresponding to the d$_{x^2-y^2}$ ground state.

For **2**, $\chi_m T$ *vs.* T plot is shown in Fig. 7. The value of $\chi_m T$
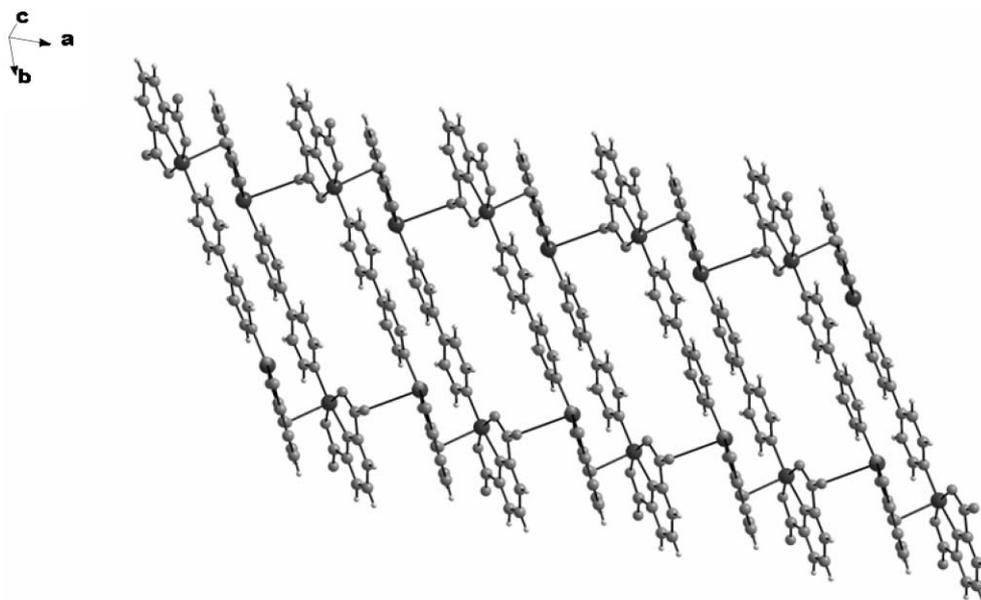
Fig. 1 A view of the propagation of the dimeric units in **1** along the crystallographic *a*-axis showing rectangular voids. Click here to access a 3D image of Fig. 1.
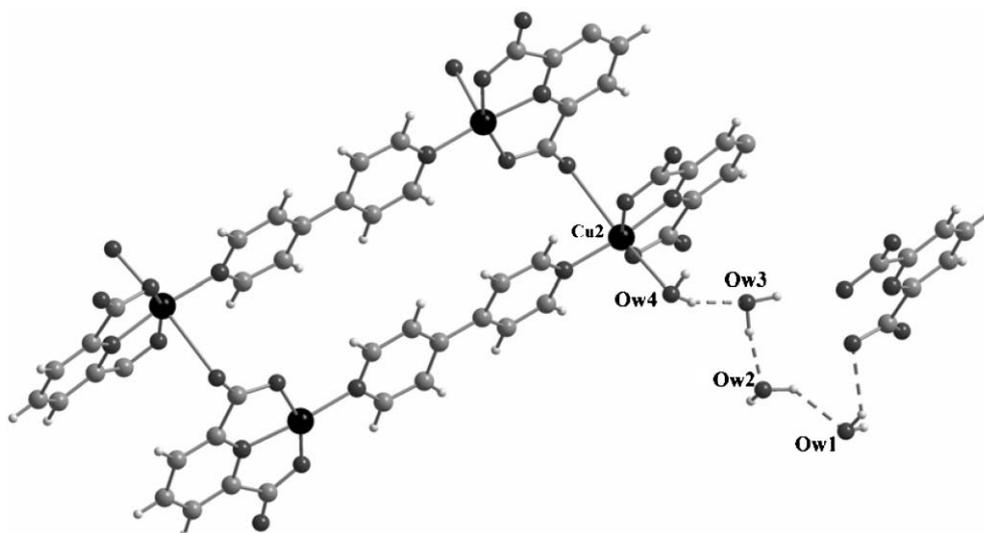

Fig. 2 Binding of acyclic water tetramers in the metal–organic framework structure in **1**.

at 300 K is 0.857 cm^3 mol^{-1} K that is again as expected for two copper ions ($g > 2.00$) which magnetically interact albeit to a very small extent. Upon cooling from 300 K, the $\chi_m T$ value remains almost constant till 60 K ; then sharply decreases as the temperature is lowered to 2 K with the final value reaching 0.20 cm^3 mol^{-1} K. The best-fit parameters calculated as in the case of **1** are: $J = -4.75 \pm 0.05$ cm^{-1}, $J' = -0.12 \pm 0.02$ cm^{-1}; $g = 2.14$ and $R = 1.2 \times 10^{-6}$. The magnetization experiment performed at 2 K between 0 and 5 T shows that the reduced molar magnetization (for the dimer) tends to 1 Nβ when the field gets 5 T (Fig. 7, inset) and it does not follow the Brillouin formula for two isolated Cu(II) ions indicative of small anti-ferromagnetic coupling. To corroborate the small J value, a full-diagonalization procedure has been used for fitting the magnetization data.[34] The best-fit values are: $J = -4.56$ cm^{-1} and $g = 2.13$. In this case it is impossible to do a fit introducing the J' parameter (intermolecular interactions). The X-band solid-state EPR spectrum of **2** shows typical axial pattern[33] with $g_\parallel = 2.25$, $g_\perp = 2.09$ corresponding to the d$_{x^2-y^2}$ ground state at 300 K which remains unchanged when cooled to 4 K.

For **3**, the plot of $\chi_m T$ *vs.* T for one copper(II) ion is illustrated in Fig. 8. The initial $\chi_m T$ value of 0.43 cm^3 mol^{-1} K, typical value for an isolated Cu(II),[31] remains almost constant till *ca.* 50 K. Then it sharply decreases to 0.20 cm^3 mol^{-1} K as the temperature is lowered to 2 K. The magnetization experiment performed at 2 K between 0 and 5 T showed that the reduced molar magnetization at 5 T is close to 1 Nβ and the curve follows the Brillouin law, assuming $g = 2.11$. So, this complex behaves as isolated copper(II) centres with a one-dimensional packing through the axial Cu–O bonds which is very long [2.793(5) Å]. Fitting of the magnetic data was carried out with the Clumag program,[35] modeling the input with 12 Cu atoms, that is the typical number taken in case of a polymeric chain. The best-fit parameters obtained with this computing model are: $J = -1.6 \pm 0.1$ cm^{-1}, $g = 2.12 \pm 0.01$ and $R = 1.2 \times 10^{-5}$. The small J value is attributable to the almost zero overlap between the ground state orbital (d$_{x^2-y^2}$) and the orbital of the bridging carboxylate O atom bound axially that propagates the polymeric chain. The X-band solid-state EPR spectra of **3** do not change with temperature (from 300 to 4 K). They show typical axial
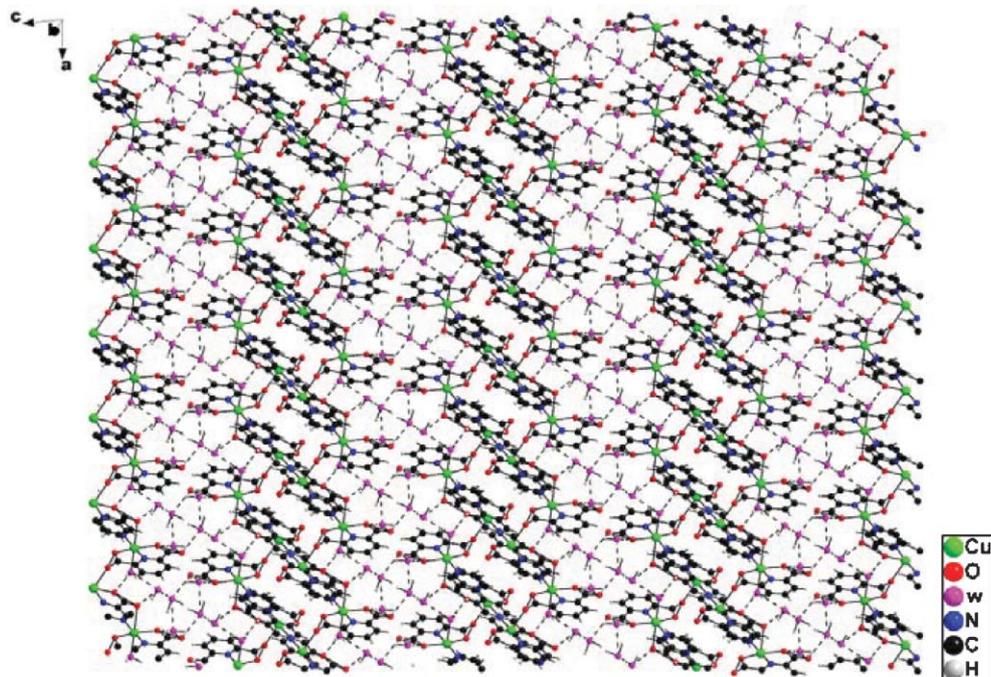
Fig. 3 A view of the open framework of **1** down the crystallographic *b*-axis showing hydrogen-bonded water molecules connecting the polymeric chains.

pattern[33] with $g_{\parallel} = 2.24$, $g_{\perp} = 2.06$ corresponding to the $d_{x^2-y^2}$ ground state.

Compound **2** shows small anti-ferromagnetic coupling; for **1** and **3**, the *J* value is significantly smaller. The difference in the anti-ferromagnetic coupling is clearly manifested either by susceptibility or magnetization measurements. In complex **2**, the bridging group between the two copper(II) ions is the pyrazine ligand. Many magnetic studies on the structurally characterized pyrazine-bridged copper(II) complexes have been reported so far.[36] Although it is not always clear if the origin of the coupling is the σ or π pathway,[36] the *J* values lies within a few wavenumbers[37] in most cases. In case of pyrazine derivatives, such as 2,3,5,6-tetra(2-pyridyl)pyrazine (TPPZ), *J* values close to -30 cm^{-1} have been reported,[38] attributable to a strong σ pathway and to the high basicity of the TPPZ ligand. Complex **1** has 4,4′-bpy as the bridging ligand with diminished magnetic interactions mainly due to the C–C single bond between the two pyridine moieties. This reduces magnetic interactions for both the σ as well as the π pathways. Thus, the introduction of this longer bridging ligand will reduce the anti-ferromagnetic coupling.[39] Indeed, the calculated *J* value for complex **1** is very small (*ca.* -1 cm^{-1}), and the corresponding *J*′, considering any possible intermolecular interactions is only *ca.* -0.1 cm^{-1}. This *J*′ is due to the polymerization of the dinuclear entities, through bridging carboxylates. The hydrogen-bonded water tetramer present in the network structure, can also contribute to this small *J*′ value (through Cu2–Ow4–Ow3–Ow2–Ow1).

Thermal gravimetric analysis of **1** with 9.85 mg sample showing onset of weight loss at 50 °C. Water removal continues up to 140 °C to give a total weight loss of 10.8% which is equivalent to losing 4H$_2$O molecules per formula unit (calcd.

Table 3 Selected atomic distances (Å) and angles (°) associated with the tetrameric water cluster

Ow4–H⋯Ow3	157.08	Ow1⋯Ow2⋯Ow3	116.93
Ow3–H⋯Ow2	171.87	Ow2⋯Ow3⋯Ow4	115.38
Ow2–H⋯Ow1	124.84		
Ow1⋯Ow2	2.778(5)	Ow1⋯Ow2⋯Ow3⋯Ow4	−117.47
Ow2⋯Ow3	2.747(5)		
Ow3⋯Ow4	2.736(6)		

value = 10.5%). The complete decomposition of the sample is achieved at 315 °C. For **2**, the analysis with 11.32 mg sample shows that the water loss starts above 80 °C and is completed at 180 °C giving a total loss of *ca.* 12% corresponding to 2H$_2$O molecules per formula unit (calcd. value $\approx$ 12%). Complete decomposition of the compound is achieved at 300 °C. Compound **3** is found to be stable up to 310 °C without any noticeable loss of weight.

Powder X-ray diffraction studies of **1** and **2** before and after water expulsion showed minor changes in the diffraction patterns attributable to robustness of the host lattices to the exclusion of water.

We have recorded FTIR spectra of **1** to characterize the vibrational stretching frequency of the O–H bond of the water cluster. The broad band centered around 3400 cm^{-1} is
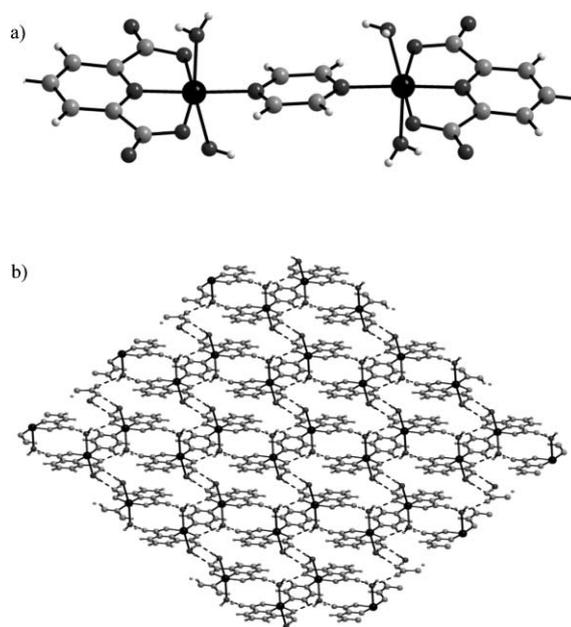

Fig. 4 (a) A perspective view of the dimeric unit in **2**. (b) An illustration showing the formation of an MOF through hydrogen bonding. Click here to access a 3D image of Fig. 4b.
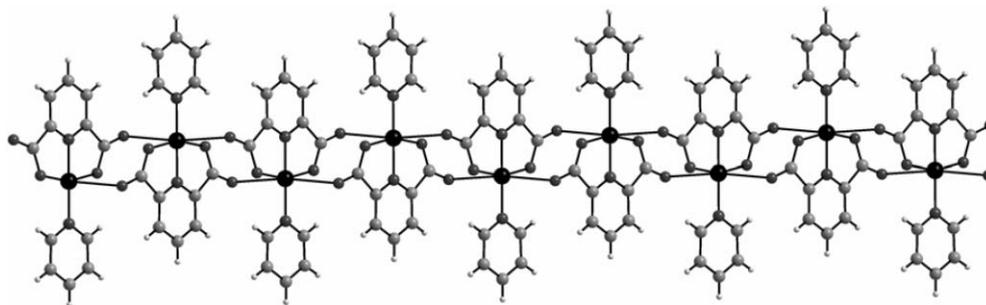
Fig. 5 The 1D coordination polymeric structure of **3** extending along the crystallographic *b*-axis. Click here to access a 3D image of Fig. 5.
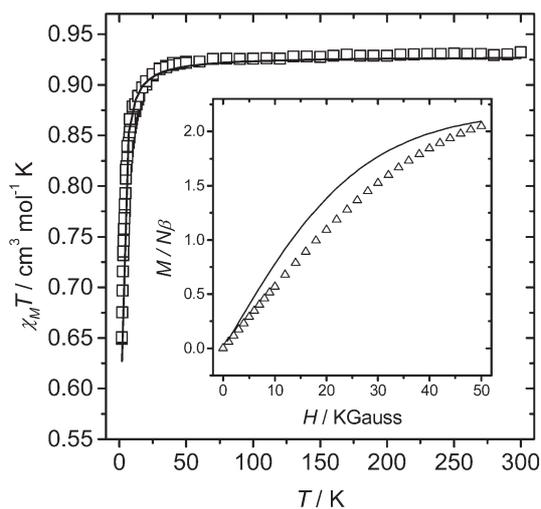

Fig. 6 Plot of the $\chi_M T$ *vs.* *T* for complex **1**. Inset: plot of the reduced magnetization of **1** at 2 K. The open point are the experimental ones and the solid lines correspond to the best fit obtained.

Fig. 8 Plot of the $\chi_M T$ *vs.* *T* for complex **3**. Inset: plot of the reduced magnetization of **3** at 2 K. The open point are the experimental ones and the solid lines correspond to the best fit obtained.

attributable[9] to the O–H stretching frequency of the water cluster. After heating the compound under vacuum (0.1 mm) at 160 °C for 2 h, the broad band disappears suggesting escape of the water molecules from the lattice. Deliberate exposure to water vapor for 3 days does not lead to re-absorption of water into the lattice as monitored by FTIR spectroscopy. The infrared spectra of **2** and **3** do not show any broad peak around 3400 cm^{-1}. However, each compound shows strong absorption
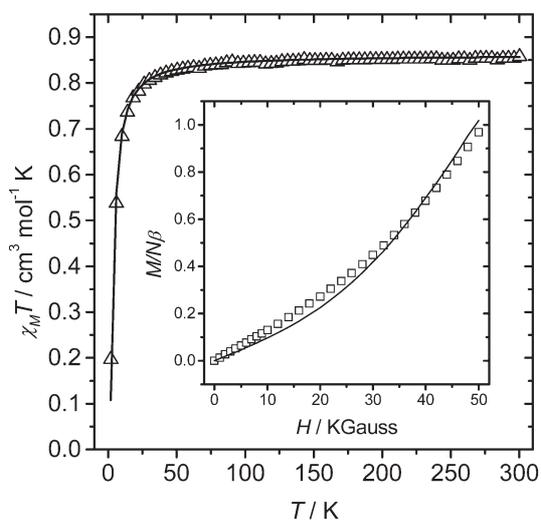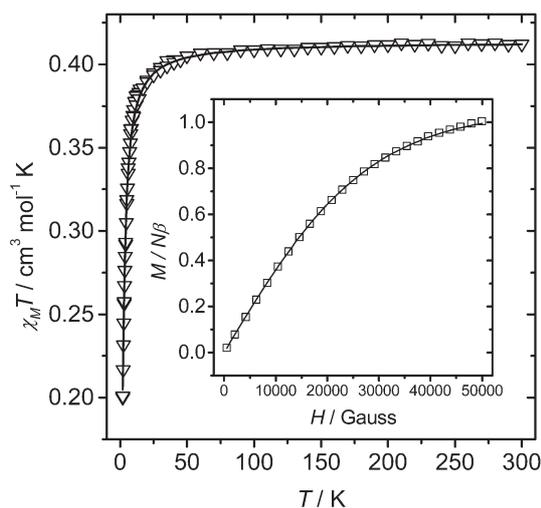
bands between 1350 and 1550 cm^{-1} diagnostic of coordinated carboxylates.[40]

Conclusion

In conclusion, we have shown that pyridine-2,6-dicarboxylate along with different spacers can form stable metal–organic framework structures of Cu(II) under hydrothermal conditions. The dimensionality of the coordination polymers could be engineered with the help of different spacers. Magnetic properties of the compounds could be rationalized based on the spacers and offers ways to make similar MOF structures with tailored magnetic properties with the ultimate aim of having molecular magnets. Size and shape of the voids created in such structures can also be manipulated by choosing different spacers. These voids can accommodate small water clusters as we have shown here for the first time, the existence of acyclic water tetramers. Studies of water clusters offer possibilities of untangling molecular details of aqueous solvation, structural stability and function of biological molecules which are largely unknown.[41]

Fig. 7 Plot of the $\chi_M T$ *vs.* *T* for complex **2**. Inset: plot of the reduced magnetization of **2** at 2 K. The open point are the experimental ones and the solid lines correspond to the best fit obtained.

References

1. M. Eddaoudi, J. Kim, N. Rosi, D. Vodak, J. Wachter, M. O'Keeffe and O. M. Yaghi, *Science (Washington, D. C.)*, 2002, **295**, 469–472.

2. (*a*) C. Boskovic, E. K. Brechin, W. E. Streib, K. Folting, J. C. Bollinger, D. N. Hendrickson and G. Christou, *J. Am. Chem. Soc.*, 2002, **124**, 3725–36; (*b*) S. A. Bourne, J. Lu, A. Mondal, B. Moulton and M. J. Zaworotko, *Angew. Chem. Int. Ed.*, 2001, **40**, 2111–13.

3. M. E. Davis, *Nature (London)*, 2002, **417**, 813–821.

4. S. S.-Y. Chui, S. M. –F. Lo, J. P. H. Charmant, A. G. Orpen and I. D. Williams, *Science (Washington, D. C.)*, 1999, **283**, 1148–50.

5. J. S. Seo, D. Whang, H. Lee, S. I. Jun, J. Oh, Y. J. Jeon and K. Kim, *Nature (London)*, 2000, **404**, 982–986.

6. H. W. Roesky and M. Andruh, *Coord. Chem. Rev.*, 2003, **236**, 91–119.

7. (*a*) O. Kahn, *Molecular Magnetism*, Wiley-VCH, New York, 1993; (*b*) J. S. Miller and A. J. Epstein, *Angew. Chem. Int. Ed.*, 1994, **33**, 385–415; (*c*) M. Ohba and H. Okawa, *Coord. Chem. Rev.*, 2000, **198**, 313–328.

8. (*a*) D. Venkataraman, G. B. Gardner, S. Lee and J. S. Moore, *J. Am. Chem. Soc.*, 1995, **117**, 11600–11601; (*b*) O. M. Yaghi, G. Li and H. Li, *Nature (London)*, 1995, **378**, 703–706; (*c*) C. J. Kepert and M. J. Rosseinsky, *Chem. Commun.*, 1999, 375; (*d*) K. Biradha, Y. Hongo and M. Fujita, *Angew. Chem. Int. Ed.*, 2000, **39**, 3843–3845; (*e*) M. Eddaoudi, D. B. Moler, H. Li, B. Chen, T. M. Reineke, M. O'Keeffe and O. M. Yaghi, *Acc. Chem. Res.*, 2001, **34**, 319–330.

9. S. K. Ghosh and P. K. Bharadwaj, *Inorg. Chem.*, 2003, **42**, 8250–8254.

10. C.-Z. Lu, C.-D. Wu, S.-F. Lu, J.-C. Liu, Q.-J. Wu, H.-H. Zhuang and J.-S. Huang, *Chem. Commun.*, 2002, 152–153.

11. (*a*) A. Fu, X. Huang, J. Li, T. Yuen and C. L. Lin, *Chem. Eur. J.*, 2002, **8**, 2239–2247; (*b*) M. Yaghi, H. Li, C. Davis, D. Richardson and T. L. Groy, *Acc. Chem. Res.*, 1998, **31**, 474–484.

12. M. Schweiger, S. R. Seidel, A. M. Arif and P. J. Stang, *Angew. Chem. Int. Ed.*, 2001, **40**, 3467–3469.

13. (*a*) R. H. Groeneman, L. R. MacGillivray and J. L. Atwood, *Inorg. Chem.*, 1999, **38**, 208–209; (*b*) D. Sun, R. Cao, Y. Liang, Q. Shi, W. Su and M. Hong, *Dalton Trans.*, 2001, 2335–2340.

14. R. Ludwig, *Angew. Chem. Int. Ed.*, 2001, **40**, 1808–1827.

15. J. L. Atwood, L. J. Barbour, T. J. Ness and C. L. Raston, *J. Am. Chem. Soc.*, 2001, **123**, 7192–7193.

16. R. Custelcean, C. Afloroaei, M. Vlassa and M. Polverejan, *Angew. Chem. Int. Ed.*, 2000, **39**, 3094–3096.

17. (*a*) J. N. Moorthy, R. Natarajan and P. Venugopalan, *Angew. Chem. Int. Ed.*, 2002, **41**, 3417–3020; (*b*) L. Infantes and S. Motherwell, *CrystEngComm*, 2002, **4**, 454–461.

18. (*a*) K. Raghuraman, K. K. Katti, L. J. Barbour, N. Pillarsetty, C. L. Barnes and K. V. Katti, *J. Am. Chem. Soc.*, 2003, **125**, 6955–6961; (*b*) A. Michaelides, S. Skoulika, E. G. Bakalbassis and J. Mrozinski, *Cryst. Growth Des.*, 2003, **3**, 487–492.

19. J. D. Cruzan, L. B. Braly, K. Liu, M. G. Brown, J. G. Loeser and R. J. Saykally, *Science (Washington, D. C.)*, 1996, **271**, 59–62.

20. F. N. Keutsch and R. J. Saykally, *Proc. Natl. Acad. Sci., U. S. A.*, 2001, **98**, 10533–10540.

21. (*a*) K. S. Kim, M. Dupois, G. C. Lie and E. Clementi, *Chem. Phys. Lett.*, 1986, **131**, 451–456; (*b*) M. Masella, N. Gresh and J.-P. Flament, *J. Chem. Soc., Faraday Trans.*, 1998, **94**, 2745–2753.

22. S. Supriya, S. Manikumari, P. Raghavaiah and S. K. Das, *New J. Chem.*, 2003, **27**, 218–220 and references therein.

23. S. Pal, N. B. Sankaran and A. Samanta, *Angew. Chem. Int. Ed.*, 2003, **42**, 1741–1743.

24. *International Tables for X-ray Crystallography*, Kynoch Press, Birmingham, UK, 1974, vol. IV.

25. A. Altomare, G. Cascarano, C. Giacovazzo and A. Gualardi, *J. Appl. Cryst.*, 1993, **26**, 343–50.

26. G. M. Sheldrick, *SHELXL-97: Program for Crystal Structure Refinement*, University of Gottingen, Germany, 1997.

27. J. Y. Lu and A. M. Babb, *Inorg. Chem.*, 2002, **41**, 1339–1341.

28. B. J. Hathaway and D. E. Billing, *Coord. Chem. Rev.*, 1970, **5**, 143–207 and references cited therein.

29. E. M. Mas, R. Bukowski and K. Szalewicz, *J. Chem. Phys.*, 2003, **118**, 4386–4403.

30. S. Dalai, P. S. Mukherjee, E. Zangrando, F. Lloret and N. R. Chaudhuri, *Dalton Trans.*, 2002, 822–823.

31. P. S. Mukherjee, S. Konar, E. Zangrando, C. Diaz, J. Ribas and N. R. Chaudhuri, *Dalton Trans.*, 2002, 3471–3476.

32. B. Bleaney and K. D. Bowers, *Proc. R. Soc. London, Ser. A*, 1952, **214**, 451–465.

33. B. J. Hathaway and D. E. Billing, *Coord. Chem. Rev.*, 1970, **5**, 143–207.

34. This program was kindly supplied by Prof. D. Gatteschi, University of Firenze, Italy, and Prof. V. Tangoulis, University of Patras, Greece.

35. CLUMAG Program: D. Gatteschi and L. G. Pardi, *Chim. Ital.*, 1993, **123**, 231–240 . This program uses a full-diagonalization procedure, employing the irreducible tensor operator (ITO) formalism.

36. H. Grove, J. Sletten, M. Julve and F. Lloret, *Dalton Trans.*, 2000, 515–522 and references therein.

37. S. Kitagawa, T. Okubo, S. Kawata, M. Kondo, M. Katada and H. Kobayashi, *Inorg. Chem.*, 1995, **34**, 4790 and references therein.

38. M. Graf, H. Stoeckli-Evans, A. Escuer and R. Vicente, *Inorg. Chim. Acta*, 1997, **257**, 89–97.

39. Y. Rodríguez-Martin, C. Ruiz-Pérez, J. Sanchis, F. Lloret and M. Julve, *Inorg. Chim. Acta*, 2001, **318**, 159–165 and references therein.

40. K. Nakamoto, *Infrared and Raman Spectra of Inorganic and Coordination Compounds*, Wiley & Sons, New York, 5th edn., 1997.

41. M. Wikström, *Curr. Opin. Struct. Biol.*, 1998, **8**, 480–488.